

Determination of flat-band position of cadmium sulfide crystals, films, and powders by photocurrent and impedance techniques, photoredox reaction mediated by intragap states

Malcolm F. Finlayson, Bob L. Wheeler, Nariyoshi Kakuta, Koon H. Park, Allen J. Bard, Alan Campion, Marye A. Fox, Stephen E. Webber, and John M. White

J. Phys. Chem., **1985**, 89 (26), 5676-5681 • DOI: 10.1021/j100272a020

Downloaded from <http://pubs.acs.org> on February 4, 2009

More About This Article

The permalink <http://dx.doi.org/10.1021/j100272a020> provides access to:

- Links to articles and content related to this article
- Copyright permission to reproduce figures and/or text from this article



ACS Publications
High quality. High impact.

tionally replaces Zn in the ZnO lattice. This model is now found to be inadequate for temperatures corresponding to those of the reaction conditions. Another mechanism must be sought.

The small Cu particle size might be important to catalytic activity. For both overheated Cu/ZnO and the catalyst prepared by impregnation the Cu particle size is large and in both cases the catalytic activity is diminished. Whether the function of ZnO is just to support the highly dispersed Cu clusters or actually to alter the electronic states of these particles for improved catalytic activity is still open to question.

CO chemisorption has been reported²¹ to have significant influences upon the structure of Rh supported on Al₂O₃ from EX-AFS studies. The CO molecule was found to strongly interact

(21) Van't Blik, H. F. J.; Van Zon, J. B. A. D.; Hizinga, T.; Vis, J. C.; Koningsberger, D. C.; Prins, R. *J. Phys. Chem.* **1983**, *87*, 2264.

also with the Cu cluster studied in this work. Under a CO atmosphere, the Cu clusters prepared by reduction at 473 K did not show any structural transformation upon lowering the temperature. Evidently chemisorption of CO has a marked effect upon the nature of the Cu cluster. Therefore, it is likely that the initial step in the catalytic synthesis of methanol is the chemisorption and activation of CO on the surface of the Cu clusters. A study of the effects of several gases upon this catalyst is now in progress and will be reported in the near future.

Acknowledgment. We express our gratitude to Mr. Shinji Kato and other staff of the Development Workshop of IMS for their collaboration in the construction of the in-situ cell used in this work. We thank Dr. Endo of IMS for the suggestions on least-squares calculations.

Registry No. ZnO, 1314-13-2; Cu, 7440-50-8; methanol, 67-56-1.

Determination of Flat-Band Position of CdS Crystals, Films, and Powders by Photocurrent and Impedance Techniques. Photoredox Reaction Mediated by Intragap States

Malcolm F. Finlayson, Bob L. Wheeler, Narioyshi Kakuta, Koon-H. Park, Allen J. Bard,* Alan Campion, Marye A. Fox, Stephen E. Webber, and John M. White

Department of Chemistry, The University of Texas, Austin, Texas 78712 (Received: April 29, 1985)

The flat-band potential of CdS has been measured for three different forms of CdS and by three different methods. Good agreement is found for determinations by Mott-Schottky and photocurrent techniques for single crystals and thin films ($V_{fb} = -1.3$ V vs. SCE in 0.1 M Na₂S). Photocurrent measurements of powder and colloidal systems yield apparent flat-band positions that are more positive than the above by about 0.7 V. The present work reveals the presence of a number of intragap states and identifies those responsible for the 0.7-V discrepancy. The effect of annealing of films and treatment of powders with Zn²⁺ on the intragap states and the improvement in CdS particle systems for H₂ evolution by ZnS coating is discussed.

Introduction

This paper deals with the energetics (band gap, band energies) of several different forms of CdS and especially with CdS powders and colloids. To decide what photoelectrochemical processes are possible at a semiconductor/liquid interface,¹ one must know the magnitude of the band-gap energy (E_{bg}), the relative energies of the band edges, and the location and density of states within the gap. E_{bg} is usually measured by spectroscopic and/or electrochemical methods. The band edges are usually located energetically by determination of the flat-band potential (V_{fb}), which can be estimated at single-crystal semiconductor electrodes by capacitance measurements (Mott-Schottky plots) or by the potential dependence of the photocurrent,² or other techniques.³ For particulate semiconductors the band edge positions have been estimated by several methods;^{3a-d} these basically involve either measuring the extent of reaction of a solution phase species as

a function of pH or direct collection of photogenerated charge at an electrode.^{3e} The presence of intragap states is inferred from luminescence measurements, studies of the impedance (particularly the conductance) of the semiconductor/liquid interface,^{4a,b} or conductivity studies.^{4c-e} A knowledge of these parameters for different forms of the semiconductor (single crystal, polycrystalline, thin film, powder, colloids) is helpful in understanding the behavior of these materials. For example, band bending, which is important for charge separation (and thus photoelectrochemical current generation) in semiconductor electrodes is not present in colloids because of their small dimensions,^{5a} and a different mechanism for charge separation in such particles has recently been postulated.^{5b} Also, since the surface/volume ratio is much greater in particles than crystals, surface and near surface states might be expected to play a more important role in the former.

One intensely studied system is CdS. Luminescence measurements of CdS in its various forms⁶ have determined that, for

(1) Wrighton, M. S. *Pure Appl. Chem.* **1985**, *57*, 1, 57.

(2) Noufi, R. N.; Kohl, P. A.; Bard, A. J. *J. Electrochem. Soc.* **1978**, *125*, 375.

(3) (a) Ellis, A. B.; Kaiser, S. W.; Bolts, J. M.; Wrighton, M. S. *J. Am. Chem. Soc.* **1977**, *99*, 9, 2839. (b) Ward, M. D.; White, J. R.; Bard, A. J. *J. Am. Chem. Soc.* **1983**, *105*, 27. (c) Dimitrijevic, N. M.; Savic, D.; Micic, O.; Nozik, A. J. *J. Phys. Chem.* **1984**, *88*, 4278. (d) Petit, J. P.; Alonso Vante, N.; Chartier, P. *J. Electroanal. Chem.* **1983**, *145*. (e) Dunn, W. W.; Aikawa, Y.; Bard, A. J. *J. Electrochem. Soc.* **1981**, *128*, 1, 222.

(4) (a) Nagasubramanian, G.; Wheeler, B. L.; Hope, G. A.; Bard, A. J. *J. Electrochem. Soc.* **1983**, *130*, 385. (b) Nicollan, E. H.; Goetzberger, A. *Bell. Syst. Tech. J.* **1967**, *46*, 1055. (c) Wright, H. C.; Downey, R. J.; Canning, J. R. *J. Phys. D.* **1968**, *1* (2) 1593. (d) Handelman, E. T.; Thomas, D. G. *J. Phys. Chem. Solids* **1965**, *26*, 1261. (e) Kulp, B. A.; Kelley, R. H. *J. Appl. Phys.* **1961**, *32*, 1290.

(5) (a) Henglein, A. In "Photochemical Conversion and Storage of Solar Energy", Rabani, J., Ed.; Weizmann Science Press of Israel: 1982; p 115. (b) Gerischer, H. *J. Phys. Chem.* **1984**, *88*, 6096.

particle sizes above 50 Å, E_{bg} (2.4 eV) is essentially independent of the physical state. Recently,⁷ E_{bg} has been shown to increase for particle sizes below about 50 Å. Our own luminescence studies of polymer encapsulated CdS⁸ also reveal the presence of intragap states at energies previously observed in single crystals, powders, and colloids. Overall, these studies suggest the presence, but not the concentrations and energetics, of intragap states.

Our interest in CdS stems from recent work in this laboratory concerning visible-light-induced hydrogen generation with small-particle CdS and ZnS semiconductors.⁹ In the case of CdS alone, H₂ is generated in the presence of a sacrificial donor, e.g. S²⁻, with very low efficiency unless Pt is also present as a catalyst for its formation. Illuminated ZnS particles have been reported¹⁰ to show H₂ formation in the absence of Pt, but the system requires ultraviolet excitation. A coprecipitated ZnS and CdS system (denoted ZnS-CdS) produces H₂ with visible light excitation at a rate comparable with platinized CdS and occurs on a variety of support materials.¹¹ Absorption and luminescence measurements of this mixed system^{8,9} show that individual CdS and ZnS phases are present rather than a solid solution. In searching for the reason why ZnS promotes the H₂ evolution ability of CdS, since ZnS is not known to act as a thermal catalyst for H₂ evolution, we investigated the possibility of a shift in the flat-band position of CdS powders on coating with ZnS. To this end we employed a photochemical method^{3b,12} which works well for band-edge measurements of particulate oxide semiconductors. As shown below, the flat-band potential (V_{fb}) of single-crystal CdS as determined from capacitance measurements^{2,3a} was approximately 0.7 V more negative than the conduction band energy obtained for silica supported CdS and unsupported CdS powders. To understand these differences and to determine the effect of CdS structure on band locations, we have investigated the behavior of single-crystal, thin-film, SiO₂-supported CdS colloids and ZnS-CdS/SiO₂ colloids and the effect of treatment with Zn²⁺ on single-crystal and thin-film electrodes.

The measurements described below are consistent with the existence of intragap states which are capable of participation in electron-transfer reactions with solution redox species. These states are responsible for the apparent difference of V_{fb} in the case of CdS particles relative to single crystals and thin films. The true flat-band position probably does not vary with form of CdS. Finally, the effect of Zn²⁺ is twofold: (a) to induce a small (~75 mV) shift in V_{fb} to more negative potentials, and (b) to block or remove surface states of CdS.

Experimental Section

1. Material Preparation. (a) Films and Crystals. Single-crystal cubic [111 face] CdS was obtained from Prof. A. B. Ellis (University of Wisconsin, Madison). Ohmic contact was made to one side of the crystal with an indium-gallium eutectic, and the electrode was then fabricated as described previously for other semiconductor single crystals.¹³ Surface cleaning was accom-

plished by etching with 6 M HCl for 15 s. Reproducible surfaces were obtained by this treatment.

Thin-film CdS electrodes were prepared by vacuum evaporation of CdS powder onto In₂O₃- and SnO₂-coated glass substrates which were cleaned as previously described.² Film thickness was estimated with a quartz thickness monitor (Sloan Technology Corp. Model DTM-3). All but a small portion (~2 mm × 3 mm) of the film was covered with paraffin wax. Contact to the film was made by an alligator clip attached to an uncoated portion of the conductive glass. A standard one-compartment electrochemical cell with an optically flat window for illumination of the electrode was used. The reference and counter electrodes were a saturated calomel electrode (SCE) and a large (~40 cm²) Pt gauze. The electrolyte in all cases was 0.1 M Na₂S in aqueous 0.2 M NaOH.

These films were annealed by heating in a He atmosphere at 400 °C for 1 h. Annealed films exhibited much greater photocurrent than nonannealed films. Annealing also served to strengthen the films and increase their robustness to insertion and removal from solution. Nonannealed films often were destroyed by this practice which was necessary for Zn²⁺ treatment. Zn²⁺ treatment was accomplished by covering the electrode surface with an aqueous (pH 7) solution of 0.01 M Zn(NO₃)₂ for 1 min followed by rinsing in distilled water.

(b) Silica-Supported Particles. CdS/SiO₂ and ZnS-CdS/SiO₂ were prepared by conventional impregnation techniques. Aqueous solutions of Cd(NO₃)₂·4H₂O and Zn(NO₃)₂·6H₂O were stirred in the presence of a suspension of silica powder (Cab-O-Sil 300 Degussa). The corresponding sulfides were precipitated on the SiO₂ particle surface upon addition of a solution of H₂S saturated water. Detailed procedures for the preparation of these catalysts are given elsewhere.¹¹ The Cd content of these supported semiconductors, as measured by treatment with HCl and atomic absorption spectroscopic analysis of the resultant solutions, yielded 24 wt % CdS in CdS/SiO₂. The term ZnS-CdS/SiO₂ refers to a coprecipitated system. ZnS and CdS in ZnS-CdS/SiO₂ were measured to be 11 and 17 wt %, respectively. All chemicals were reagent grade and were used as received. Colloidal solutions were afforded by sonication of the SiO₂ supported particles.

2. Measurements. (a) Photocurrents. Two types of photocurrent measurements were employed: one, employing MV²⁺ as a mediating electron acceptor (for the particles) and a second, direct method for films and crystals. In the first case^{3b,12} the colloidal solution was irradiated in the presence of MV²⁺ and Na₂S (0.1 M). Photoexcited electrons from the conduction band reduce MV²⁺ to MV^{•+} while holes from the valence band oxidize S²⁻ to ¹/₂S₂²⁻. MV^{•+} is reoxidized at a platinum electrode and the resultant current measured. In the present case, since there is a substantial dark current at high pH from thermal reduction of the viologen by Na₂S, the initial slope (photocurrent/time) rather than the absolute magnitude of the photocurrent was used. This method has been previously described in detail for unsupported CdS particles^{12a} and In₂O₃ semiconductor particles.^{12b}

In the second method, anodic photocurrent was measured directly for the single-crystal and thin-film systems (without MV²⁺). The CdS electrodes, immersed in 0.1 M Na₂S, were placed directly in the modulated (PAR Model 192 chopper operating at 87 Hz) output of an Oriel 450-W Xe lamp. The lamp was equipped with an IR water filter and an Oriel 370-nm long-pass spectral filter. Light intensity at the electrode surface, measured with a radiometer (EG and G Model 550), was 70 mW cm⁻².

Current-voltage curves were generated by a PAR 173 potentiostat with PAR 175 programmer and an XYY recorder (Soltech Model 6432). Phase-sensitive photocurrent curves employed lock-in detection with a PAR Model 5204 lock-in amplifier. The magnitude and phase angle outputs of the lock-in output were recorded.

(b) Impedance Techniques. The apparatus and procedures have previously been described.⁴ A small (12-mV p-p) sinusoidal voltage was superimposed on the linear voltage ramp from the

(6) (a) Ramsden, J.; Graetzel, M. J. *Chem. Soc., Faraday Trans. 1* **1984**, *80*, 919. (b) Halsted, R. E.; Aven, M.; Coghill, H. D. *J. Electrochem. Soc.* **1965**, *112*, 177. (c) Ibuki, S.; Ohso, A. *J. Phys. Chem. Solids* **1966**, *27*, 1753. (d) Ellis, A. B.; Karas, B. R. *Adv. Chem. Ser.* **1980**, *No. 184*, 185. (e) Harzion, Z.; Huppert, D.; Gottsfeld, S. *J. Electroanal. Chem.* **1983**, *571*. (f) Shiraki, Y.; Shimadi, T.; Komatsubara, K. F. *J. Appl. Phys.* **1974**, *45*, 3554. (g) Wendel, G. *Fortschr. Phys.* **1953**, *1*, 45.

(7) (a) Brus, L. E. *J. Chem. Phys.* **1984**, *80*, 1. (b) Rossetti, R.; Nakahara, S.; Brus, L. E. *J. Chem. Phys.* **1983**, *79*, 1086. (c) Rossetti, R.; Ellison, J. L.; Gibson, J. M.; Brus, L. E. *J. Chem. Phys.* **1984**, *80*, 4464. (d) Nozik, A. J.; Williams, F.; Nenadovic, M. T.; Rajh, T.; Micic, O. I. *J. Phys. Chem.* **1985**, *89*, 397.

(8) Finlayson, M. F.; Park, K. H.; Katuta, N.; Bard, A. J.; Campion, A.; Fox, M. A.; Webber, S. E.; White, J. M., manuscript in preparation.

(9) Ueno, A.; Kakuta, N.; Park, K. H.; Finlayson, M. F.; Bard, A. J.; Campion, A.; Fox, M. A.; Webber, S. E.; White, J. M. *J. Phys. Chem.* **1985**, *89*, 732.

(10) Reber, J. F.; Meier, K. *J. Phys. Chem.* **1984**, *88*, 5903.

(11) Ueno, A.; Kakuta, N.; Park, K. H.; Finlayson, M. F.; Bard, A. J.; Campion, A.; Fox, M. A.; Webber, S. E.; White, J. M., manuscript in preparation.

(12) (a) White, J. R.; Bard, A. J. *J. Phys. Chem.* **1985**, *89*, 1947. (b) Erbs, W.; Kiwi, J.; Graetzel, M. *Chem. Phys. Lett.* **1984**, *110*, 648.

(13) Wheeler, B. L.; Nagasubramanian, G.; Bard, A. J. *J. Electrochem. Soc.* **1984**, *131*, 2289.

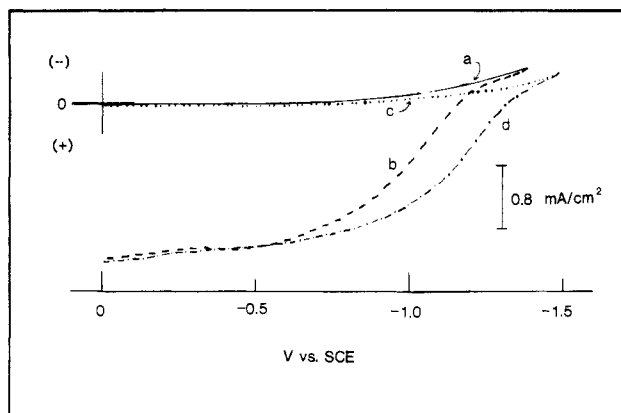


Figure 1. Current-potential behavior of single-crystal n-CdS in 0.1 M Na_2S -0.2 M NaOH solution: (a) etched electrodes in dark, (b) same electrode under illumination, (c) Zn^{2+} treated electrode in dark, (d) same electrode under illumination.

potentiostat. The in-phase and 90° out-of-phase components of the dark current were measured as a function of applied potential. The quadrature component yields the capacitance. Capacitance-voltage plots were used to obtain V_{fb} for single crystals and thin films. The in-phase component (conductance) is sensitive to the presence of surface and bulk states.⁴

Thin-film ac impedance measurements revealed intraband-gap states both of a surface and subsurface nature. The frequency dependence of the conductance was used to characterize further one of these states. To obtain the equivalent parallel conductance (G) as a function of frequency, a PAR 5206 lock-in amplifier with internal oscillator option and a MINC-11 computer (DEC) for data acquisition were used in conjunction with the potentiostat and programmer.

(c) *Hydrogen Generation.* The SiO_2 supported semiconductor powder (50 mg) was suspended in 12 mL of 0.1 M Na_2S . The suspension was sonicated under vacuum in a glass vial fitted with a rubber septum. Irradiation employed a 450-W Xe lamp equipped with a water jacket and a Corning 3-72 long-pass filter. Light intensity at the sample surface was 30 mW/cm^2 . The rubber septum permitted intermittent gas removal by syringe. The gas above the liquid was analyzed by gas chromatography (Varian Model 90-p). N_2 was used as carrier gas and no gas other than hydrogen was detected. The techniques have previously been described.⁹

Results and Discussion

1. *Band Position Measurements.* (a) *Single Crystals.* Dark and photocurrents vs. applied electrode potential curves were obtained for single-crystal CdS, both untreated (Figure 1, a and b) and following surface treatment with Zn^{2+} (Figure 1, c and d). The photocurrent onset potential for the etched clean surface is -1.39 V vs. SCE . This agrees well with the value (-1.34 V vs. SCE) found from Mott-Schottky plots in the dark of these electrodes under identical conditions, as illustrated by the upper rightmost point in Figure 2. There are three effects caused by Zn^{2+} treatment (Figure 1): (1) the photocurrent rises more sharply after the onset; (2) the onset potential is shifted approximately 80 mV more negative, and (3) the dark current is decreased.

(b) *Colloids.* Determination of E_c , the location of the conduction band edge, in this experiment rests on the fact that the solution redox potential of the $\text{MV}^{2+/+}$ couple ($E_{\text{redox}} = -0.69 \text{ V vs. SCE}$) is pH independent whereas E_c is not (Figure 2). When the CdS Fermi level, E_f , lies at more negative values than -0.69 V vs. SCE , conduction band electrons may reduce MV^{2+} . Photocurrent is first noticeable in this system when E_f lies at about the same potential as the viologen couple (the quasi-Fermi level lies very close to the conduction band level, E_c , for heavily doped n-type semiconductors and under intense illumination). At lower pH values, reduction of the viologen will not occur, since the conduction band edge now lies positive of E_{redox} .

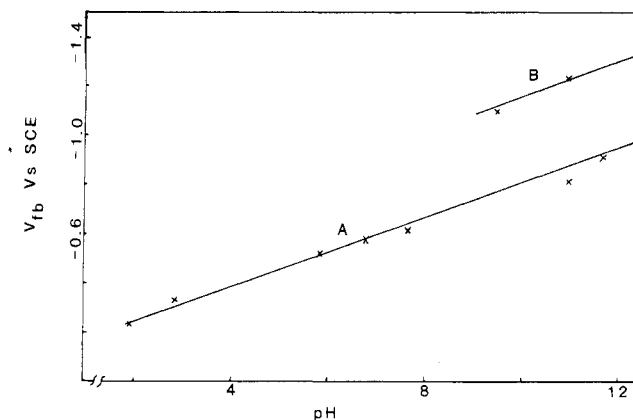


Figure 2. pH dependence of V_{fb} for the CdS single crystal as determined from $1/C^2$ vs. V plots: (A) without Na_2S , (B) in 0.1 M Na_2S .

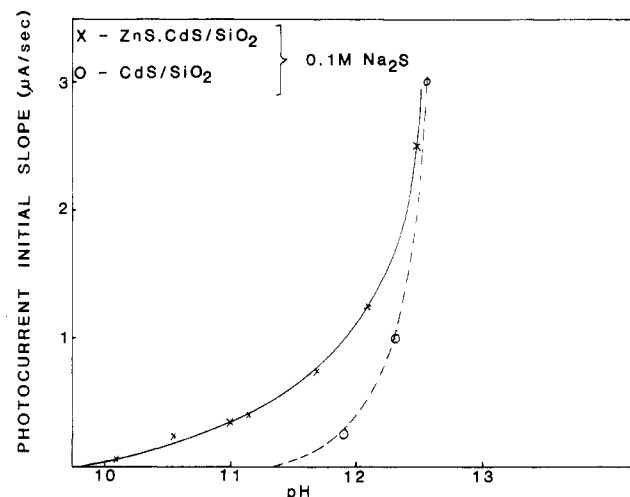


Figure 3. Initial photocurrent slope vs. pH of photoinduced reduction of MV^{2+} in 0.1 M Na_2S by (a) colloidal CdS/ SiO_2 and (b) colloidal ZnS-CdS/ SiO_2 .

Figure 3 shows a plot of the initial photocurrent increase vs. pH for the photoinduced reduction of MV^{2+} by colloidal CdS/ SiO_2 and colloidal ZnS-CdS/ SiO_2 . Recent studies of the photocurrent on unsupported CdS particles^{12a} in the presence of MV^{2+} show an almost identical pH for photocurrent onset and a shift in the apparent V_{fb} of approximately 50 mV/pH unit. The Mott-Schottky data for the single crystals also showed V_{fb} to shift in a negative direction with increasing pH (70 mV/pH, Figure 2). The SiO_2 support therefore does not affect the apparent V_{fb} . From the present photocurrent measurements the "apparent" V_{fb} for CdS/ SiO_2 is -0.74 V vs. SCE (pH 12.5, 0.1 M Na_2S). Note that this value is more than 0.5 V more positive than that of the single crystal. Note also that the positive pH shift of the photocurrent onset of ZnS-CdS/ SiO_2 compared with that of CdS/ SiO_2 (Figure 3) corresponds to a negative shift in the apparent V_{fb} of 70 mV in the former. The effect of Zn^{2+} on the single crystal surface is thus very similar to the effect of ZnS interacting strongly with CdS and suggests that Zn^{2+} treatment may result in the formation of ZnS on the surface.

(c) *Thin Films.* Plots of photocurrent vs. applied electrode potential for thin (9000 Å) CdS films are presented in Figure 4. For nonannealed films (Figure 4, curve a), the photocurrent was small relative to the large dark currents and phase-sensitive detection was mandatory.

Treatment of a nonannealed film with 0.01 M $\text{Zn}(\text{NO}_3)_2$ improved the saturation photocurrent by a factor of 2 (Figure 4, curve b). Film annealing without Zn^{2+} treatment increased the photocurrent by a factor of 20 (Figure 4, curve c). Annealed films exhibited lower dark currents and greatly improved photocurrents which could easily be measured by dc methods. However, the phase-sensitive photocurrent is shown in Figure 4 for comparison

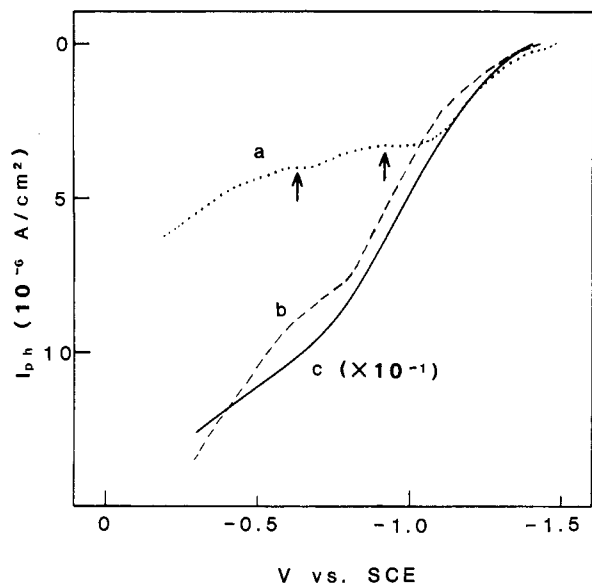


Figure 4. Phase-sensitive photocurrent-voltage curve for CdS thin-film electrodes in 0.1 M Na₂S-0.2 M NaOH: (a) as-deposited film, (b) Zn²⁺ treated film, (c) annealed film.

with nonannealed films. Zn²⁺ treatment of the annealed films did not improve the photocurrent any further. Note that for these films the onset of photocurrent occurs at -1.36 V for both annealed and Zn²⁺ treated films, and -1.43 V vs. SCE for nonannealed films. Within experimental error (± 0.1 V), these duplicate the V_{fb} position found from the Mott-Schottky plots of the single crystals under the same conditions. Note that, in the case of CdSe films, Zn²⁺ treatment also induces a negative shift in V_{fb} ¹⁶ and yields an improved fill factor.

2. Intragap States. One must address the question of the difference in apparent flat-band potentials of the particles vs. the single crystals and thin films of CdS. Moreover, the beneficial effects of the Zn²⁺ treatment in terms of photocurrent onset and H₂ evolution (on the particles) must be considered. As discussed below, we propose that intragap states are responsible for these effects.

(a) Thin-Film Photocurrent. In the photocurrent-voltage curves for the nonannealed CdS films (Figure 4, curve a), there are two small humps, indicated by arrows. These humps, which were reproducible and always appeared with thin CdS films, are attributed to electron/hole recombination sites or traps that reduce the magnitude of photocurrent. These traps are only partially removed by the Zn²⁺ treatment (Figure 4, curve b). These results point to a set of states distributed in energy (we refer to these as A states). The annealed films showed only a smoothly increasing photocurrent with increasing reverse bias.

Evidence for these states was also found in the impedance measurements. As discussed previously¹³ measurement of the out-of-plane (C, capacitance) and in-phase (G, conductance) signals as a function of potential and angular frequency (ω) can provide information about the energy and density of intragap surface states.

(b) Impedance Behavior—High Frequency. Capacitance values obtained from high-frequency (200–1000 Hz) ac impedance data gave Mott-Schottky plots which yielded V_{fb} values for the thin CdS films which agreed only sometimes with the phase-sensitive photocurrent onset potentials. However, interpretation of such plots is not straightforward, since the plots show frequency dispersion in both slope and intercept. This type of behavior has previously been observed in CdS² and CdSe¹⁴ films.

(c) Impedance Behavior—Low Frequency. Besides the A states discussed above, we have observed and characterized another set

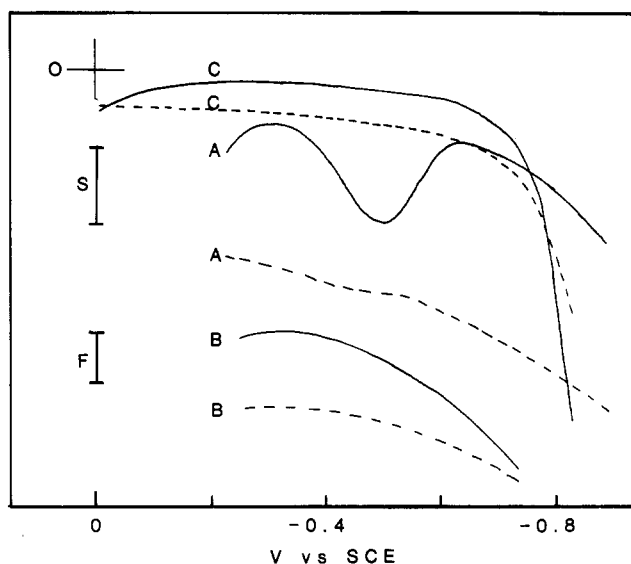


Figure 5. ac impedance of CdS in 0.1 M Na₂S-0.1 M NaOH: conductance (0° component, solid line) and capacitance (90° component, dashed line). F = conductance scale (mho), S = capacitance scale (μ F). (A) Nonannealed (9000 Å) film: $F = 1 \times 10^{-5}$, $S = 1$. (B) Annealed thin film: $F = 5 \times 10^{-6}$, $S = 0.3$. (C) Single-crystal CdS: $F = 1 \times 10^{-6}$, $S = 0.05$.

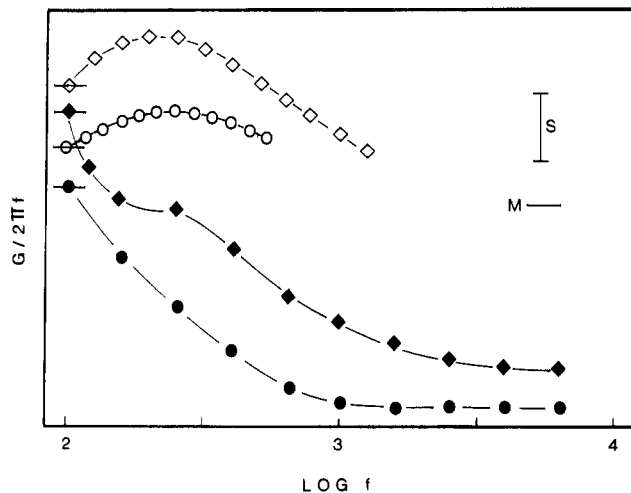


Figure 6. Frequency dependence of the conductance (G) for the various forms of CdS in 0.1 M Na₂S-0.1 M NaOH. S = scale, M = origin on abscissa. (A) Nonannealed film (open circles): $S = 6.5 \times 10^{-6}$, $M = 1.4 \times 10^{-6}$. (B) Annealed thin film (full circles): $S = 6.5 \times 10^{-6}$, $M = 3.4 \times 10^{-6}$. (C) Etched single crystal (open diamond): $S = 1.5 \times 10^{-4}$, $M = 5.2 \times 10^{-6}$. (D) Zn²⁺ treated single crystal (full diamond): $S = 1.5 \times 10^{-5}$, $M = 6.4 \times 10^{-6}$.

of intragap states for the films. These latter states (B states) appear to reside in the bulk since they are also unaffected by surface Zn²⁺ treatment. Figure 5 illustrates the in-phase (G) and quadrature (C) components of the current resulting from the superimposed ac voltage. For nonannealed thin (9000 Å) film CdS (curves A) a minimum clearly occurs in the in-phase (G) component at -0.5 V vs. SCE. Annealing the film completely removes these states (curves B), and they were not observed on etched single crystals (curves C). Again, this observation was independent of the nature of support material. Such minima have previously^{14,15} been shown to indicate the presence of surface states or traps in the space-charge region. Since Zn²⁺ treatment does not remove the minimum, the states probably penetrate to the bulk. From the relationship^{4a,b,15} $G/\omega = (C_{ss}\omega\tau)/(1 + \omega^2\tau^2)$, where C_{ss} is the surface state capacitance, and τ is the time constant associated with carrier exchange, it is possible to estimate τ . A plot (at a given potential) of G/ω vs. f , where $\omega = 2(\pi)f$ and f is the ac frequency in Hz, will exhibit a maximum at $\omega\tau = 1$. Therefore, $\tau = 1/\omega$ at this maximum. Such plots are presented in Figure

(14) Reichman, J.; Russak, M. A. *J. Appl. Phys.* **1982**, *53*, 708.

(15) Nagasubramanian, G.; Wheeler, B. L.; Bard, A. J. *J. Electrochem. Soc.* **1983**, *130*, 1680.

(16) Reichman, J.; Russak, M. A. *J. Electrochem. Soc.* **1981**, *128*, 2025.

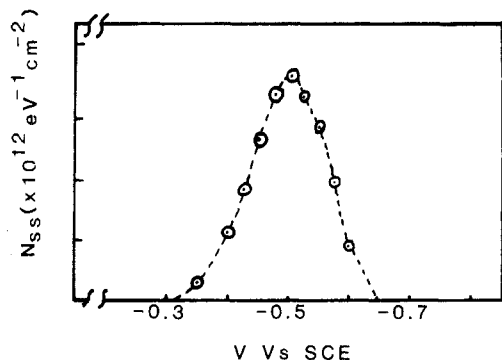


Figure 7. Density of B states as a function of applied electrode potential.

6. A value of $600 (\pm 100) \mu\text{s}$ was obtained in this manner. This long time constant is not unreasonable, since time constants for intragap states generally increase with increasing separation from the band edges. The B states lie approximately in the middle of the CdS band gap and communication with the band edges which lie more than 1 eV away is not expected to be good.

The number of states at any given potential can be estimated from the relationship $N_s = 2G\tau/e$,^{4a,b} where G is the parallel equivalent conductance (in-phase component) and τ is the time constant described above. A plot of state density vs. applied potential is given in Figure 7. Integration of this plot gives an estimate of the total density of states within this potential regime as $6 \times 10^{11} \text{ cm}^{-2}$.

Annealing the film completely removes the hump from the G vs. voltage (Figure 5, curve b) and G/ω vs. f plots (Figure 6, full circles). G/ω vs. f plots for single-crystal CdS (Figure 6, open diamonds) at a bias of -0.5 V vs. SCE also show a peak at the same frequency as the thin-film CdS, even though low-frequency G vs. voltage plots of the same crystals (Figure 5, curve c) exhibited no minima. Freshly etched, then Zn^{2+} treated, CdS single crystals showed a shoulder but no clear hump at the same frequency (Figure 6, full diamonds) indicating that these states reside at least partially on the surface.

(d) *Intragap States and Solution Redox Species.* Thus far we have identified two sets of intragap states (A and B) that act as electron-hole recombination sites. We propose that these states are capable of participating in electron transfers to solution species and are responsible for the apparent difference in V_{fb} between thin film/single crystals and powder/colloid systems, i.e., that electron transfer to MV^{2+} from the particulate CdS occurs not from the conduction band but rather from states lying within the band gap. We attribute the beneficial effect of the Zn^{2+} treatment on the H_2 evolution reaction to arise from partial passivation of these states. Consider the energy scheme depicted in Figure 8, where the relative energies of states are plotted in V vs. SCE. In this diagram the band energies are based on V_{fb} and E_g measurements, and the intragap states (labeled as arrows) on the photocurrent and impedance measurements (probably with an experimental error of $\pm 0.1 \text{ V}$). This model is also consistent with previous studies involving particulate CdS systems. For example, in a recent study of CdS luminescence,^{6a} electron transfer from states within the band gap has been observed. In this study MV^{2+} , RuO_2 , and RuS_2 quenched the red (subband gap) emission of CdS particles very efficiently. In the case of MV^{2+} , a new emission was induced at higher energy and was attributed to the formation of cadmium vacancies. In the cases of RuO_2 and RuS_2 , the red emission was quenched very efficiently whereas the band-gap recombination (515 nm) emission was not. This quenching of the red luminescence can be attributed to direct charge transfer from this emitting state to MV^{2+} as opposed to nonpopulation of this emitting state by scavenging of conduction band electrons. We have also observed MV^{2+} quenching of the red but not the green luminescence of CdS⁸ in polymer films so that site-specific interaction of MV^{2+} with CdS appears general.

The A states are at energies where MV^{2+} reduction can occur in 0.1 M Na_2S . Since photochemistry mostly occurs from the lowest-lying levels of a given manifold, reduction of MV^{2+} by

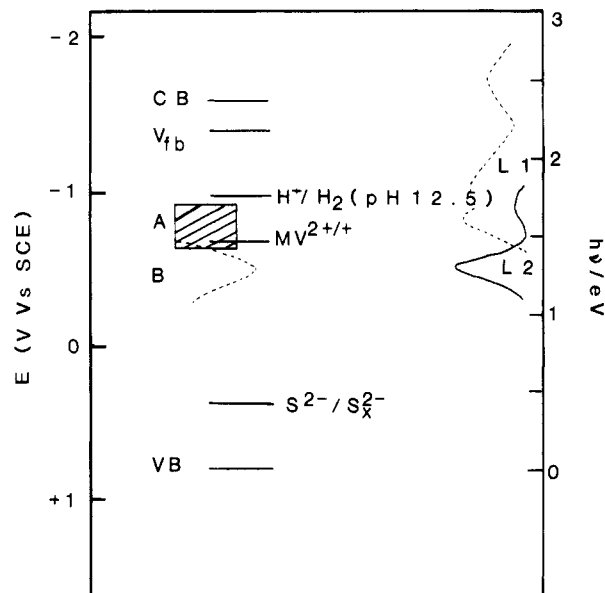


Figure 8. Energy diagram from CdS in the dark, in contact with 0.1 M Na_2S -0.2 M NaOH solution. Electron potential energy is increasing upward. For reference, the electrochemical potential scale vs. SCE is included: CB, conduction band edge; VB, valence band edge; V_{fb} , flat-band potential; A, B, recombination traps observed in this work; L1, L2, luminescent states.

electrons in the A states would yield an apparent V_{fb} of about -0.7 V vs. SCE ; this is very close to the "apparent V_{fb} " value measured in the MV^{2+} photocurrent experiment with particulate systems. Also, since Zn^{2+} treatment does not completely remove the A states, the value of V_{fb} measured in the same manner for $\text{ZnS}\cdot\text{CdS}/\text{SiO}_2$ is not very different from CdS/ SiO_2 . Again this is in keeping with the experimental result. The A states are thus identified as the states responsible for the apparently low value of V_{fb} in the powder system. The B states lie too low to be of importance for electron transfer to MV^{2+} but could conceivably be involved in other charge-transfer processes.

(e) *Intragap States and Luminescence.* Photoluminescence in CdS has been observed to occur within the range 600–850 nm,^{3a,6} and these transitions can be identified with transitions from the proposed states. We assume that electrons produced by excitation above E_{bg} fall to the lower states and emission results from transitions from these to the valence band.^{3a} In this way the red luminescent region may be located in Figure 8 (dotted line labeled L1). This luminescent region overlaps the A states observed in the present study and is tentatively assigned to the latter. Emission from these states is partially quenched by addition of Zn^{2+} ⁸ and further supports this assignment, since we observe the same phenomenon electrochemically (Figure 4, curve b). CdS photoluminescence has also been observed in the region 850–1020 nm.¹⁷ If we assume this transition again to originate in intragap states and terminate in the valence band, these states may also be located in Figure 8 (labeled L2). These "luminescent states" clearly overlap the B states observed in the present study. The data of Figure 7, plotted on the same scale, and normalized to the luminescence maximum, give the dashed curve on the left in Figure 8; the width of this band is similar to that of the luminescence. The B states are thus tentatively assigned to those responsible for the luminescence L2. Electroluminescence¹⁷ of CdS also involves emission in both L1 and L2 regions, consistent with these same assignments. These emissions^{6f} as well as edge emissions^{6g} are eliminated upon annealing at 400°C and these results are in complete agreement with the electrochemical observations reported here. To our knowledge, this is the first time that electrochemically located intragap states have been directly correlated with luminescent states in the same system.

(17) Nakato, Y.; Tsumura, A.; Tsubomura, H. *Chem. Phys. Lett.* **1982**, 55, 387.

(f) *Intragap States and Hydrogen Production.* We ascribe the increased activity toward hydrogen production of ZnS-CdS over CdS to (a) the small induced negative shift in the apparent V_{fb} and (b) the blocking of surface states by Zn^{2+} . Removal of these pathways for electron/hole recombination must necessarily increase the fraction of electrons available at more negative potentials for H_2 production, i.e., any electrons in the conduction band will have a greater reducing power than those within the band gap. The luminescence intensity from states closer to the conduction band is thus expected to increase in the presence of Zn^{2+} and we have observed⁸ such enhancement. When ZnS coats CdS, hydrogen production is improved over the case where CdS coats ZnS.^{9,11} This shows the importance of both (a) and (b) above, since both effects are operative for CdS/ZnS whereas only (a) can operate in ZnS/CdS. This proposed modification and passivation of surface states by treatment with metal ion is similar to that observed previously with semiconductor electrodes. For example, treatment of n-type GaAs with Ru^{3+} has been shown to improve its efficiency as a photoanode and this has been ascribed to surface state passivation.¹⁸ Similarly, the performance of photoanodes such as WSe_2 has been improved by appropriate surface treatments.¹⁹ We note that Zn^{2+} treatment has previously been reported to reduce CdS dark currents.²⁰

By annealing films in an He atmosphere, A and B are apparently more completely removed, and the photocurrent increased by a factor of 20. Photocurrent and hydrogen production ability generally parallel each other. We therefore hoped that increased hydrogen production would result when the particles were annealed. However, heating either CdS/SiO₂ or ZnS-CdS/SiO₂ at 400 °C in a He atmosphere (for up to 4 h) failed to increase their activity toward H_2 production with respect to the nonannealed particles. This failure of heat treatment to improve the activity of the particles is likely due to the different nature of films and particles. It may be very difficult to anneal surface states from small particles in which a large fraction of the material is on or near the surface. The case of CdSe films¹⁶ may be analogous. CdSe films deposited at low substrate temperatures (below 200 °C) were amorphous, peeled easily from the substrate, and showed

poor I-V characteristics. As noted earlier, we found identical behavior with our "as-deposited" CdS films. Heat treatment of CdSe (400 °C, air, 15 min) benefitted the films in a manner identical with our CdS films. In the case of CdSe,¹⁶ heat treatment converted the amorphous material to crystalline (hexagonal) form. The similarity with CdS behavior suggests a similar situation. In the case of ZnS-CdS particles, however, electron diffraction⁹ clearly shows that CdS already exists in a crystalline (cubic) state prior to heat treatment. Annealing the particles at 400 °C did not alter the crystallinity and therefore did not improve the photoelectrochemical properties.

Concerning the site of H_2 production in the ZnS-CdS system, we believe Cd metal to be involved. In work to be published elsewhere²¹ we show that metallic cadmium is formed upon visible light irradiation of ZnS-CdS but not upon visible light irradiation of CdS. Metallic zinc was not observed following irradiation of ZnS-CdS.

Conclusions

There is no significant dependence of V_{fb} on the state or form of CdS, nor on the nature of support material.

The intragap and surface states observed in this study can play a role in observed photoprocesses, such as photoinduced hydrogen production for either CdS/SiO₂ or ZnS-CdS/SiO₂.

Measurements by photoinduced electron transfer from particles to solution acceptor species may not yield the actual V_{fb} , since electron transfer from intragap states may occur. Measurements of this type with a graded set of pH independent redox couples might be useful in determining the number and importance of intragap redox active surface states in powder and colloidal semiconductor systems.

The enhancement of hydrogen production in the mixed ZnS-CdS semiconductor particulate system results from apparent V_{fb} shifts to more negative potentials with resultant Cd metal formation and blocking of surface states by Zn^{2+} which lowers the number of recombination sites.

Acknowledgment. The financial support of this research by the Gas Research Institute (No. 5982-260-0756) is gratefully acknowledged.

Registry No. MV^{2+} , 4685-14-7; CdS, 1306-23-6; ZnS, 1314-98-3; Na_2S , 1313-82-2; SiO₂, 7631-86-9; Zn, 7440-66-6; H_2 , 1333-74-0.

(21) Kakuta, N.; Park, K. H.; Ueno, A.; Finlayson, M. F.; Bard, A. J.; Campion, A.; Fox, M. A.; Webber, S. E.; White, J. M., manuscript in preparation.

(18) Parkinson, B. A.; Heller, A.; Miller, B. *Appl. Phys. Lett.* **1978**, *33*, 6, 521.

(19) (a) White, H. S.; Abruna, H. D.; Bard, A. J. *J. Electrochem. Soc.* **1982**, *129*, 265. (b) White, H. S.; Fan, F.-R. F.; Bard, A. J. *J. Electrochem. Soc.* **1981**, *128*, 1045.

(20) (a) Tenne, R. *Ber. Bunsenges. Phys. Chem.* **1981**, *85*, 413. (b) Neumann-Spallart, M.; Kalyanasundaram, K. *Ber. Bunsenges. Phys. Chem.* **1981**, *85*, 1112.

Phosphine and Its Coadsorption with D₂O on Rh(100)

C. M. Greenlief, R. I. Hegde, and J. M. White*

Department of Chemistry, University of Texas at Austin, Austin, Texas 78712 (Received: July 9, 1985)

The interaction of PH_3 with Rh(100) has been investigated by X-ray photoelectron and ultraviolet photoelectron spectroscopies. Even at 100 K on Rh(100) and 25 K on Ni(100), the adsorption of PH_3 is partly dissociative. Adsorbed phosphorus and phosphine are readily distinguished by XPS. Molecular and dissociated PH_3 can be distinguished in UPS. Coadsorption studies show no evidence for H-D exchange between D_2O and PH_3 . Preadsorbed D_2O partially inhibits PH_3 dissociation. The He II UPS spectra of multilayer PH_3 , measured at 25 K, are readily correlated with existing gas-phase data.

Introduction

The surface chemistry of adsorbed phosphorus-containing molecules is largely unexplored. Recently, we have reported the study of the adsorption of dimethylmethylphosphonate (DMMP) on Rh(100).¹ We have also examined the surface chemistry of

PH_3 on Rh(100) by Auger electron spectroscopy (AES) and temperature-programmed desorption (TPD).² In another recent study, Hegde and White³ have used TPD to probe the effects of coadsorbed H_2 , D_2 , O_2 , and H_2O with PH_3 on Rh(100).

(1) R. I. Hegde, C. M. Greenlief, and J. M. White, *J. Phys. Chem.*, **89**, 2886 (1985).

(2) R. I. Hegde, J. Tobin, and J. M. White, *J. Vac. Sci. Technol. A*, **3**, 339 (1985).

(3) R. I. Hegde and J. M. White, *Surf. Sci.*, **157**, 17 (1985).